Arch. Mech., 40, 1, pp. 17–24, Warszawa 1988

Nonproportional loading tests, tensile torsion ratchetting, at elevated temperature, of a 316L austenitic stainless steel (17-12 SPH)

P. DELOBELLE, C. LEXCELLENT and C. OYTANA (BESANÇON)

The aim of this paper is to compare the predictions of a model already described [1, 2], and identified for an austenitic stainless steel 17–12 SPH, (with uniaxial tensile (1D) and proportional biaxial tensile-torsion (2D) tests) to non-proportional loading experiments. More precisely the longitudinal ratchetting of tubes, induced by torsional cycling under constant tensile stress is considered. Thus, the first part report some experimental results obtained on the quoted alloy, in a second part a qualitative comparison with the model predictions and possibilities is described.

Celem pracy jest porównanie rezultatów teoretycznych wynikających z opisanego w pracach [1, 2] modelu nierdzewnej stali austenitycznej 17–12 SPH (poddanej próbom jednoosiowego rozciągania oraz dwuosiowego rozciągania ze skręcaniem) z wynikami doświadczeń przy obciążaniu nieproporcjonalnym. Rozważono więc problem kumulacji odkształceń wzdłużnych próbek rurkowych poddanych cyklicznemu skręcaniu i stałemu rozciąganiu. W pierwszej części pracy omówiono szereg wyników eksperymentalnych dotyczących omawianego stopu, w części drugiej przeprowadzono jakościowe porównanie tych wyników z wynikami analizy rozważanego modelu.

Целью работы является сравнение теоретических результатов, вытекающих из описанной в работах [1, 2] модели нержавеющей аустенитной стали 17–12 SPH (подвергнутой испытаниям одноосного растяжения и двухосевого растяжения со скручиванием), с результатами экспериментов при непропорциональном нагружении. Итак, рассмотрена проблема кумуляции деформаций продольных трубчатых образцов, подвергнутых циклическому скручиванию и постоянному растяжению. В первой части работы обсужден ряд экспериментальных результатов, касающихся обсуждаемого сплава, а во второй части проведено качественное сравнение этих результатов с результатами анализа рассматриваемой модели.

1. Experimental results

THE TESTS were performed on a creep tensile-torsion device with servo and cam controlled stresses and having large stiffness. This device is associated with an accurate extensometry allowing long term and reliable measurements [3]. The experimental sequence of the reported tests consisted in a small axial tensile loading ($\sigma_{zz} = 50$ MPa) and then in a cyclic superposed shear strain with a constant amplitude ($\varepsilon_{z\vartheta_t} = \pm 0.35\%$) with a fixed shear strain rate $\dot{\varepsilon}_{z\vartheta} = 4 \cdot 6\ 10^{-5}\ s^{-1}$. This type of loading was performed at various temperatures T and the cumulated tensile strain ε_{zz} was got versus the number of cycles N (Fig. 1) together with the simultaneous shear stress $\sigma_{z\vartheta}$ hardening (Fig. 2). As will be further seen, the shapes of the curves $\varepsilon_{z\vartheta} = f(\varepsilon_{zz})$ and $\sigma_{z\vartheta} = f(\varepsilon_{z\vartheta})$ give conclusive information about the ratchetting origin and therefore a definite help to its modelling [4].

The main following observations must be pointed out:

i) The cumulative strain is a logarithmic function of the cycles number N.

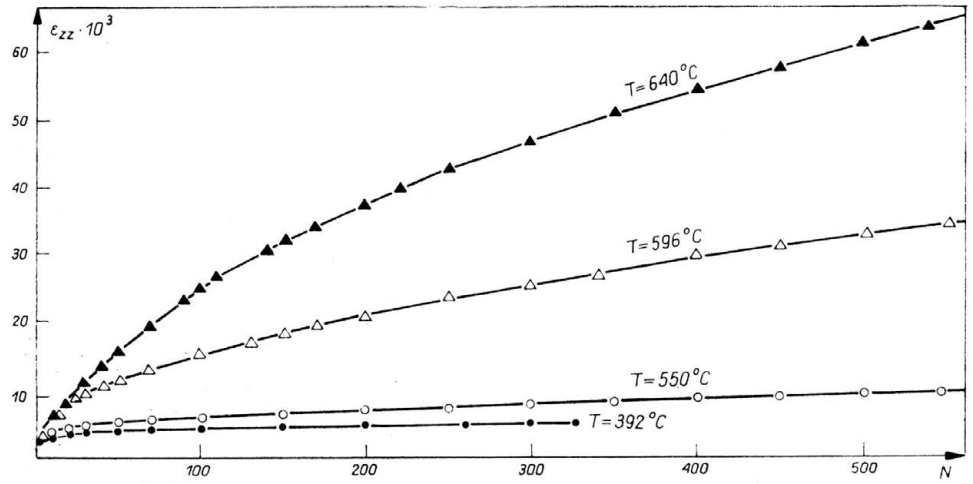

FIG. 1. Cumulated ratchetting axial strain versus the number of shear cycles for 4 different temperatures: $T = 640°C$, $596°C$, $550°C$, $392°C$, $\sigma_{zz} = 50$ MPa; $\varepsilon_{z\vartheta t} = \pm 0.35 \times 10^{-2}$; $\dot{\varepsilon}_{z\vartheta} = 4.6 \times 10^{-5}$ s^{-1}.

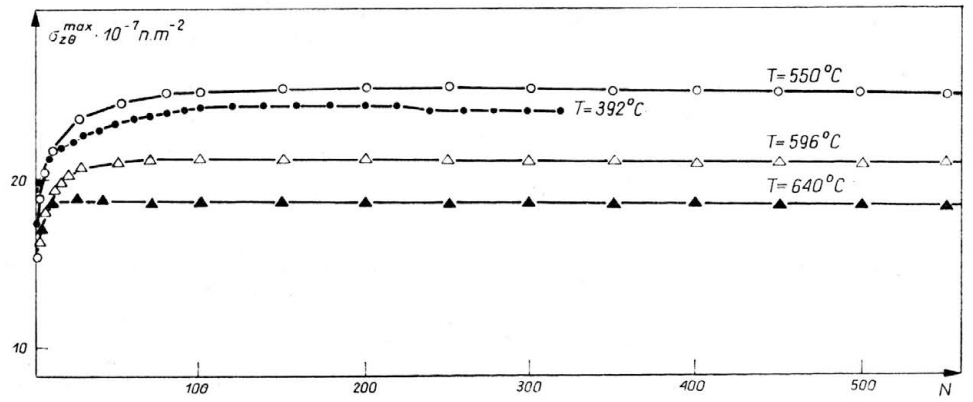

FIG. 2. Evolution of the torsion shear stress $\sigma_{z\vartheta}$ in the experiments of Fig. 1 (cyclic hardening).

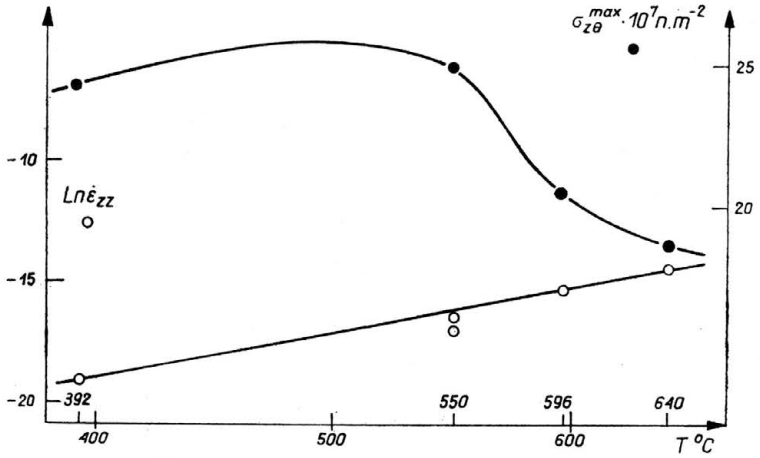

FIG. 3. Evolution of $\dot{\varepsilon}_{zz}$ and of stabilized $\sigma_{z\vartheta}^{st}$ versus temperature T.

ii) The geometric ratchetting, i.e. that obtained at zero tensile stress is quite weak ($\varepsilon_{zz} \simeq 10^{-3}$ for $N = 300$) when compared to the one induced by first order flow rules in the cases of a nonzero σ_{zz}.

iii) For a given N value, the longitudinal strain rate $\dot{\varepsilon}_{zz}$ depends only slightly on temperature: the apparent activation energy is about 0.5 e.V. (Fig. 3), while creep activation

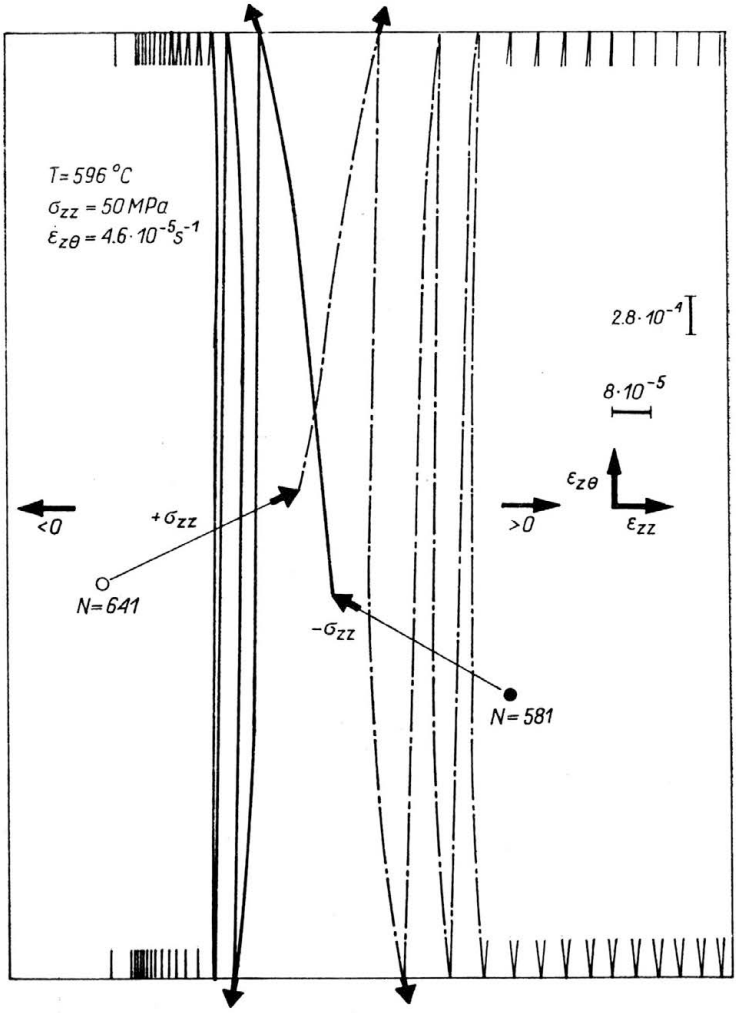

FIG. 4. Shape of the curves $\varepsilon_{z\vartheta} = f(\varepsilon_{zz})$ corresponding: a) to complete negative stress decrement ($\sigma_{zz} = -\Delta\sigma_{zz}$) (negative ratchetting) at $N = 581$. b) after an increment of stress equal at σ_{zz} at $N = 641$ (positive ratchetting).

energy lies about 5 e.V. [1]. In a similar way the saturation $\sigma_{z\vartheta}$ value for large N decreases when T increases (Figs. 2 and 3).

iv) When, after about 600 cycles, the tensile stress is removed through a σ_{zz} decrease $\Delta\sigma_{zz}$, with $\Delta\sigma_{zz} = \sigma_{zz}$, a negative ratchetting occurs ($\varepsilon_{zz} \simeq 10^{-3}$ after 100 consecutive cycles at $T = 600°C$) and must be associated with a change in the $\varepsilon_{zz} = f(\varepsilon_{z\vartheta})$ curves

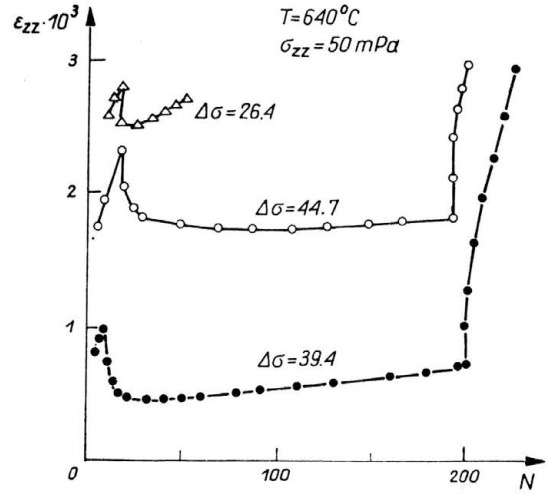

FIG. 5. Axial ratchetting responses to $\Delta\sigma_{zz}$ negative stress drops. Occurrence of successively negative, zero and positive cumulative axial strains in the curves ε_{zz} versus $(N)_T$, for various $\Delta\sigma_{zz}$.

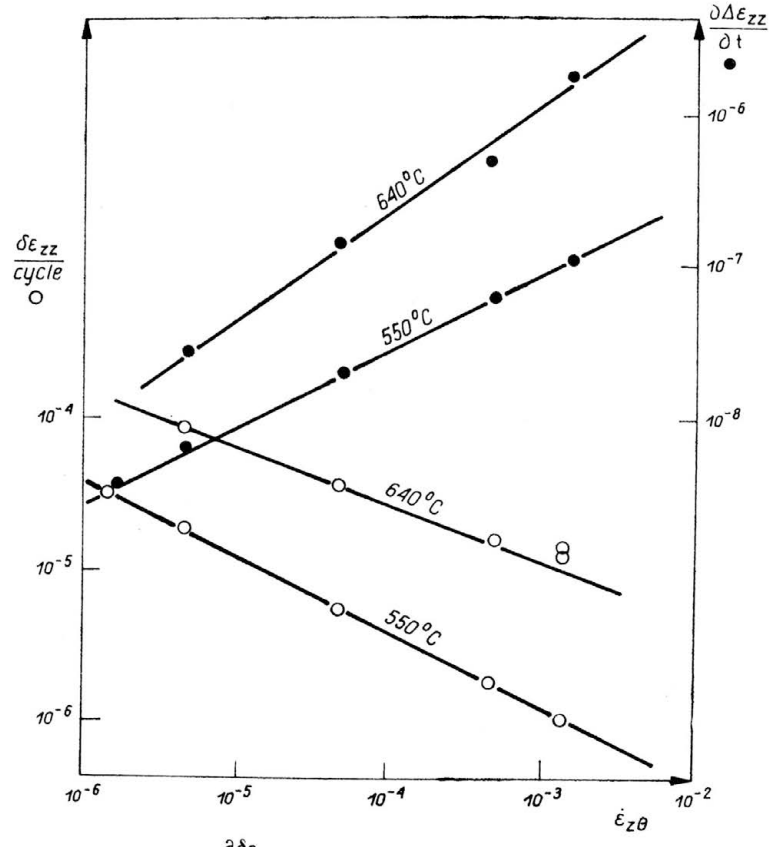

FIG. 6. Evolution of $\dot{\varepsilon}_{zz} = \dfrac{\partial \delta \varepsilon_{zz}}{\partial t}$ and $\delta\varepsilon_{zz}$ cycle with the imposed shear strain rate $\dot{\varepsilon}_{z\theta}$.

concavity, i.e. these curves are concave when $\dot{\varepsilon}_{zz} > 0$ and are convex when $\dot{\varepsilon}_{zz} < 0$ (Fig. 4).

The points iii) and iv) support the usual assumption that ratchetting phenomena are related to the rule of orthogonality of the strain flow either to equipotential surfaces (viscoplastic case) or to limit surfaces (plastic case).

v) If a partial $\Delta\sigma_{zz}$ drop leading to a new value of tensile test $(\sigma_{zz}-\Delta\sigma_{zz})$ is realized, a negative ratchetting period follows even for small drop magnitudes. This period is the longer, the larger is $\Delta\sigma_{zz}$ and is followed by a new positive ratchetting, (Fig. 5) the rate of which is close to that which would have been obtained by a direct axial loading to $(\sigma_{zz}-\Delta\sigma_{zz})$ at the same N value. This shows that the recovery of the substructure and of the associated internal variables is active even at the lowest experimental temperatures ($T = 550°C$).

vi) If, for the same type of loading, the imposed shear strain rate $\dot{\varepsilon}_{z\vartheta}$ is increased by a large amount (this was done with $\dot{\varepsilon}_{z\vartheta}$ from 1.4×10^{-6} s^{-1} to 1.4×10^{-3} s^{-1}), the tensile strain rate $\dot{\varepsilon}_{zz}$ increases while the ratchetting magnitude per cycle, $\partial\varepsilon_{zz}/\partial N$, is drastically decreased (factor $\simeq 35$) (Fig. 6). Therefore the ratchetting strain, at high temperature, $500 \leqslant T \leqslant 650°C$, is essentially viscous.

2. Comparison with a model based on proportionnel loadings

To describe tensile tests and proportionnal biaxial tensile-torsion tests, we proposed a unified viscoplastic model, the main characteristics of which are:

i) There is a single viscoplastic state equation $\bar{\dot{\varepsilon}} = f(\overline{\sigma-\alpha})$ where, $\dot{\varepsilon}_{ij}$, σ_{ij} and α_{ij} being, respectively, the strain rate components, the applied stress components and a tensorial kinematical variable, we have:

$$\bar{\dot{\varepsilon}} = \sqrt{\frac{2}{3}}\,(\dot{\varepsilon}_{ij}\dot{\varepsilon}_{ij})^{1/2}, \qquad \overline{\sigma-\alpha} = \sqrt{\frac{3}{2}}\,\{(\sigma'_{ij}-\alpha'_{ij})\,(\sigma'_{ij}-\alpha'_{ij})\}^{1/2},$$

σ'_{ij} and α'_{ij} being the deviatoric components of σ and α. The function f is strongly nonlinear, what makes it possible to obtain time dependent and time quasi-independent strains.

ii) The viscoplastic equipotentials then give strain rate components

$$\dot{\varepsilon}_{ij} = \frac{3}{2} f(\overline{\sigma-\alpha})\,\frac{\sigma'_{ij}-\alpha'_{ij}}{\overline{\sigma-\alpha}}.$$

iii) Active loadings give large strains while unloadings produce small strains; this is accounted for by a criterion depending on the internal variable α.

iv) On the unloading side of the criterion and in the tensile (or compression) uniaxial case, $\alpha = \alpha_1$, α_1 exhibiting a large strain hardening h_0. On the other side, during active loadings, $\alpha = \alpha_2 + Y$ with the corresponding H_{α_2} and H_Y hardening parameters such that $H_Y + H_{\alpha_2} \ll h_0$. In this case $\alpha_1 = \alpha$ is imposed to α_1.

v) Steady creep appears during tests and this is accounted for by recovery terms introduced in the evolution rules of α_1, α_2 and Y.

vi) The criterion is written as: $\overline{\alpha_1-\alpha_2} = Y$, $(\overline{\alpha_1-\alpha_2})$ is the second invariant of the tensor $(\alpha_1-\alpha_2)$ when complex stress states are considered. In Fig. 7 (a and b), the double space of the stresses and of the internal variables is represented. Thus the equipotential surfaces centered at $\{\alpha\} = \{\alpha_1\}$ are drawn as full line circles; they are related to the stress space and govern the strain rate direction. For instance, point A corresponds to the stress tensor $(\sigma)_1$ and, at this point, the strain rate direction is orthogonal to the circle centered at B (the representative point of $\{\alpha_1\}_1$) and passing through A.

On the other hand, the active loading-unloading criterion has a limit surface in the internal variables space represented by the dashed circle centered at $\{\alpha_2\}_1$ with a radius: $\overline{\alpha_1-\alpha_2} = Y$. The consistency equations must prevent $\{\alpha_1\}$ from lying outside the criterion limit surface (i.e. $\overline{\alpha_1-\alpha_2} > Y$ is impossible). In Fig. 7, the criterion corresponding to point A and a proportional loading (for which $\{\alpha_2\}_1$ colinear to $\{\alpha_1\}_1$) is reported.

a)

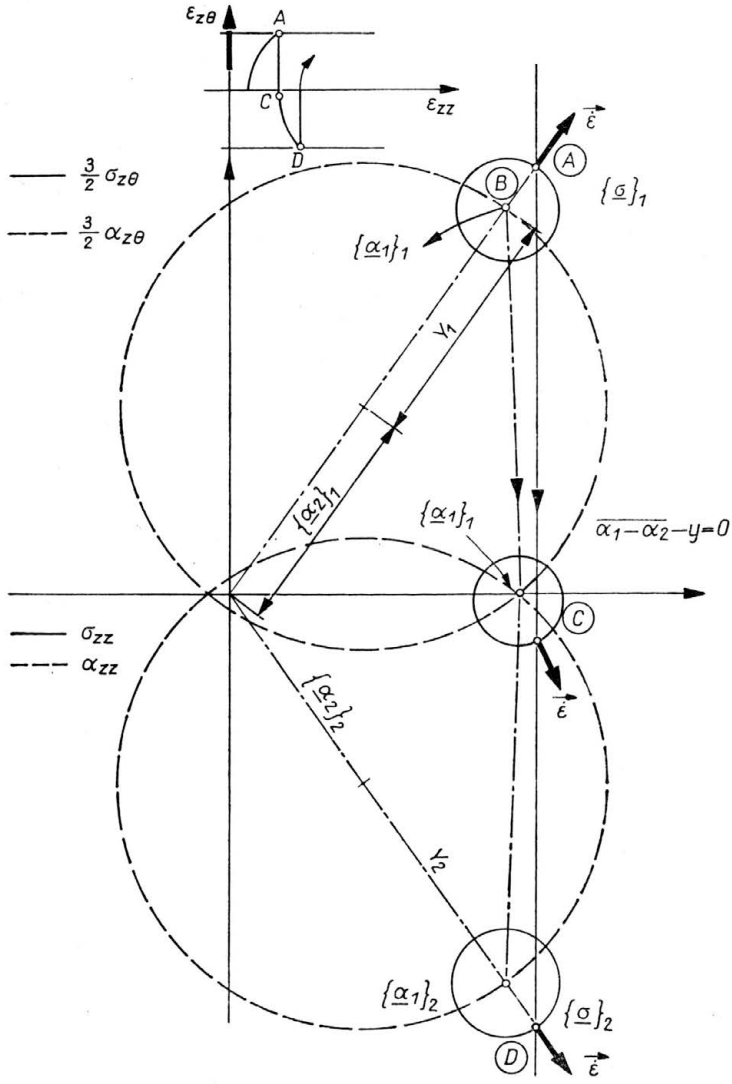

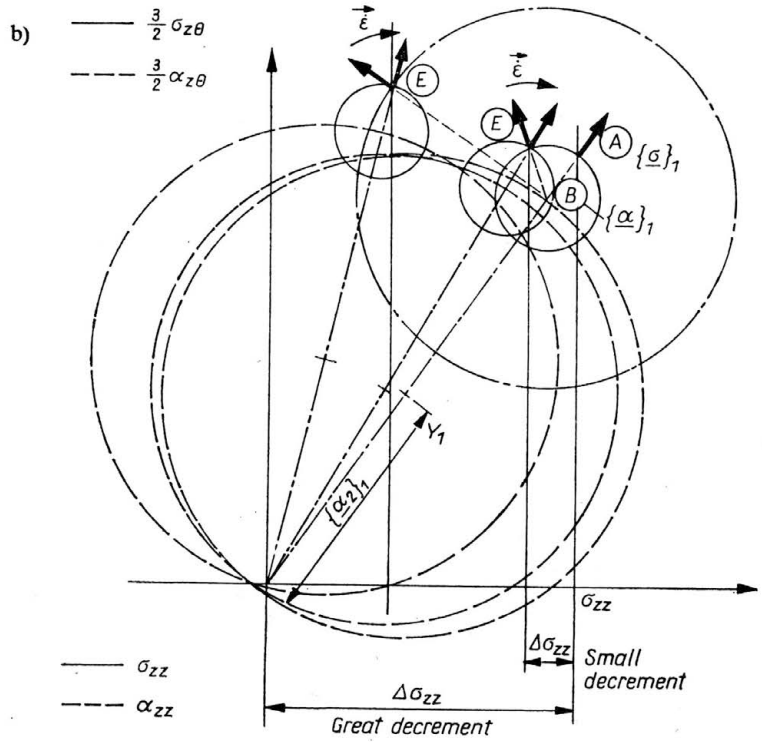

FIG. 7. Qualitative prediction of the experimental observations. a) When $\dot{\varepsilon}_{z\theta}$ changes its sign. b) For a decrement $\Delta\sigma_{zz}$ (state just after the decrement and stabilized state).

Now, let us consider the case of our experiments; to make the description simpler, Y will be assumed to be constant. If starting from point A, $\varepsilon_{z\theta}$ is cycled, $\sigma_{z\theta}$ decreases ($|\dot{\varepsilon}_{z\theta}|$ being imposed) and tends towards $-\sigma_{z\theta}$ in the steady state. When $\sigma_{z\theta}$ decreases from A, microviscoplastic strains are obtained (microviscoplastic strains are those produced in unloading situations). As h_0 is very large, $\{\alpha\} = \{\alpha_1\}$ keeps close to the applied stress $\{\sigma\}$ and a small positive axial strain is got (a limit example is given by an infinite h_0 in which case no plastic strain is produced and the criterion becomes $\overline{\sigma - \alpha_2} = Y$). This situation holds on until a point close to C is reached and $\overline{\alpha_1 - \alpha_2} = Y$ is obtained. Then, the following decrease of $\sigma_{z\theta}$ results in macroviscoplastic strains (those corresponding to active loading cases). The strain rate direction is orthogonal to the circle centered at $\{\alpha_1\}$ and passing through C. The ratchetting of axial strain is still small and positive. As the $\sigma_{z\theta}$ decrease goes on, one tends to the situation described by D, the criterion limit surface has shifted from $\{\alpha_2\}_1$ to $\{\alpha_2\}_2$.

At D ratchetting is larger as orthogonality to the circle centered at $\{\alpha_1\}_2$ and passing through $\{\sigma\}_2$ gives a larger longitudinal strain rate component. The upper left curve of Fig. 7a shows the resulting effect.

Let us now consider another type of experiment (Fig. 7b). In A, during a test, a small tensile stress decrease $\Delta\sigma_{zz}$ is produced and is such that $\sigma_{zz} - \alpha_{zz} - \Delta\sigma_{zz} < 0$, due again to the orthogonality of the flow directions to a circle which just after the drop is still centered

at A; a negative $\dot{\varepsilon}_{zz}$ is obtained during the consecutive cycling of $\varepsilon_{z\vartheta}$. The center of the flow equipotentials is no longer in A and thus in E the tensile negative strain component may be large (Fig. 7b). During the cycling α_{zz} decreases and when $\sigma_{zz}-\Delta\sigma_{zz}-\alpha_{zz} = 0$ no longitudinal ratchetting can be produced. A new positive axial ratchetting demands that internal variables recovery be active to make $\sigma_{zz}-\Delta\sigma_{zz}-\alpha_{zz} > 0$. (We present in Fig. 7b two cases of small and great decrements). Therefore the model derived and identified from proportional loading allows for qualitative predictions of the nonproportional ratchetting effects described here; this includes the important observation of a negative ratchetting following a small decrease of σ_{zz}. Quantitative comparison can therefore be continued.

References

1. P. DELOBELLE, Thesis, 1–302, Besançon 1985.
2. P. DELOBELLE, C. OYTANA, 5th Int. Sem. on: "Inelastic Analysis and Life Prediction in High Temperature Environment", Paris 1985, Rue Louis Murat Paris VIIIe, C. Baylac, A. S. Ponter and F. Leckie, EDF Septem., pp. 69–102, 1985.
3. P. DELOBELLE, D. VARCHON, Rev. Phys. Appl., **18**, 667, 1983.
4. P. BLANCHARD, J. TORTEL, 5th Int. Sem. on "Inelastic Analysis and Life Prediction in High Temperature Environment", pp. 125–186, August 26–27, Paris 1985.

LABORATOIRE DE MECANIQUE APPLIQUEE, ASSOCIE AU CNRS
FACULTE DES SCIENCES ET DES TECHNIQUES DE BESANÇON, FRANCE.

Received July 30, 1986.

Arch. Mech., 40, 1, pp. 17–24, Warszawa 1988

Nonproportional loading tests, tensile torsion ratchetting, at elevated temperature, of a 316L austenitic stainless steel (17-12 SPH)

P. DELOBELLE, C. LEXCELLENT and C. OYTANA (BESANÇON)

The aim of this paper is to compare the predictions of a model already described [1, 2], and identified for an austenitic stainless steel 17–12 SPH, (with uniaxial tensile (1D) and proportional biaxial tensile-torsion (2D) tests) to non-proportional loading experiments. More precisely the longitudinal ratchetting of tubes, induced by torsional cycling under constant tensile stress is considered. Thus, the first part report some experimental results obtained on the quoted alloy, in a second part a qualitative comparison with the model predictions and possibilities is described.

Celem pracy jest porównanie rezultatów teoretycznych wynikających z opisanego w pracach [1, 2] modelu nierdzewnej stali austenitycznej 17–12 SPH (poddanej próbom jednoosiowego rozciągania oraz dwuosiowego rozciągania ze skręcaniem) z wynikami doświadczeń przy obciążaniu nieproporcjonalnym. Rozważono więc problem kumulacji odkształceń wzdłużnych próbek rurkowych poddanych cyklicznemu skręcaniu i stałemu rozciąganiu. W pierwszej części pracy omówiono szereg wyników eksperymentalnych dotyczących omawianego stopu, w części drugiej przeprowadzono jakościowe porównanie tych wyników z wynikami analizy rozważanego modelu.

Целью работы является сравнение теоретических результатов, вытекающих из описанной в работах [1, 2] модели нержавеющей аустенитной стали 17–12 SPH (подвергнутой испытаниям одноосного растяжения и двухосевого растяжения со скручиванием), с результатами экспериментов при непропорциональном нагружении. Итак, рассмотрена проблема кумуляции деформаций продольных трубчатых образцов, подвергнутых циклическому скручиванию и постоянному растяжению. В первой части работы обсужден ряд экспериментальных результатов, касающихся обсуждаемого сплава, а во второй части проведено качественное сравнение этих результатов с результатами анализа рассматриваемой модели.

1. Experimental results

THE TESTS were performed on a creep tensile-torsion device with servo and cam controlled stresses and having large stiffness. This device is associated with an accurate extensometry allowing long term and reliable measurements [3]. The experimental sequence of the reported tests consisted in a small axial tensile loading ($\sigma_{zz} = 50$ MPa) and then in a cyclic superposed shear strain with a constant amplitude ($\varepsilon_{z\vartheta_t} = \pm 0.35\%$) with a fixed shear strain rate $\dot{\varepsilon}_{z\vartheta} = 4 \cdot 6\ 10^{-5}\ s^{-1}$. This type of loading was performed at various temperatures T and the cumulated tensile strain ε_{zz} was got versus the number of cycles N (Fig. 1) together with the simultaneous shear stress $\sigma_{z\vartheta}$ hardening (Fig. 2). As will be further seen, the shapes of the curves $\varepsilon_{z\vartheta} = f(\varepsilon_{zz})$ and $\sigma_{z\vartheta} = f(\varepsilon_{z\vartheta})$ give conclusive information about the ratchetting origin and therefore a definite help to its modelling [4].

The main following observations must be pointed out:

i) The cumulative strain is a logarithmic function of the cycles number N.

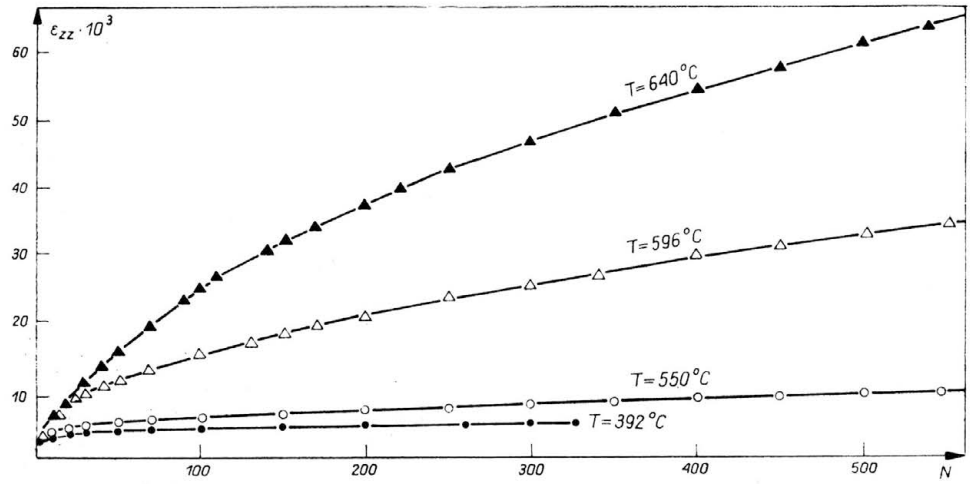

FIG. 1. Cumulated ratchetting axial strain versus the number of shear cycles for 4 different temperatures: $T = 640°C$, $596°C$, $550°C$, $392°C$, $\sigma_{zz} = 50$ MPa; $\varepsilon_{z\vartheta t} = \pm 0.35 \times 10^{-2}$; $\dot{\varepsilon}_{z\vartheta} = 4.6 \times 10^{-5}$ s^{-1}.

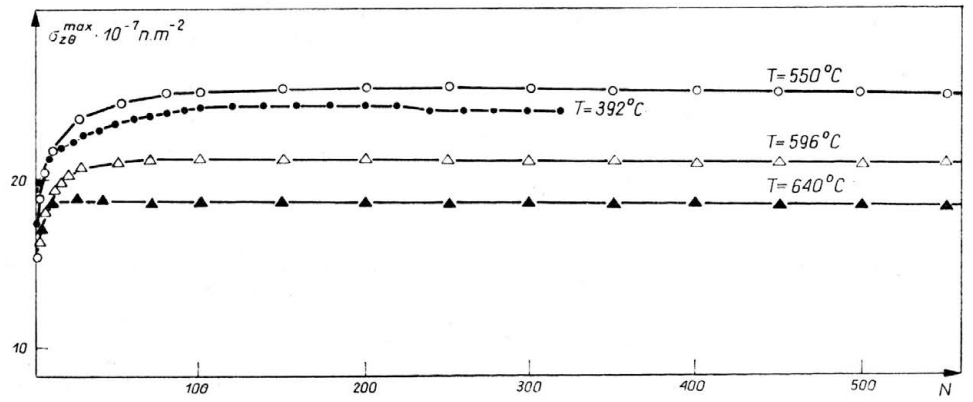

FIG. 2. Evolution of the torsion shear stress $\sigma_{z\vartheta}$ in the experiments of Fig. 1 (cyclic hardening).

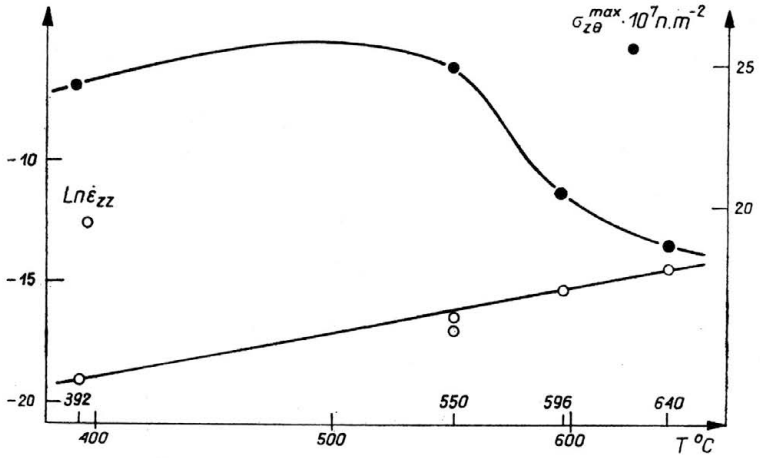

FIG. 3. Evolution of $\dot{\varepsilon}_{zz}$ and of stabilized $\sigma_{z\vartheta}^{st}$ versus temperature T.

ii) The geometric ratchetting, i.e. that obtained at zero tensile stress is quite weak ($\varepsilon_{zz} \simeq 10^{-3}$ for $N = 300$) when compared to the one induced by first order flow rules in the cases of a nonzero σ_{zz}.

iii) For a given N value, the longitudinal strain rate $\dot{\varepsilon}_{zz}$ depends only slightly on temperature: the apparent activation energy is about 0.5 e.V. (Fig. 3), while creep activation

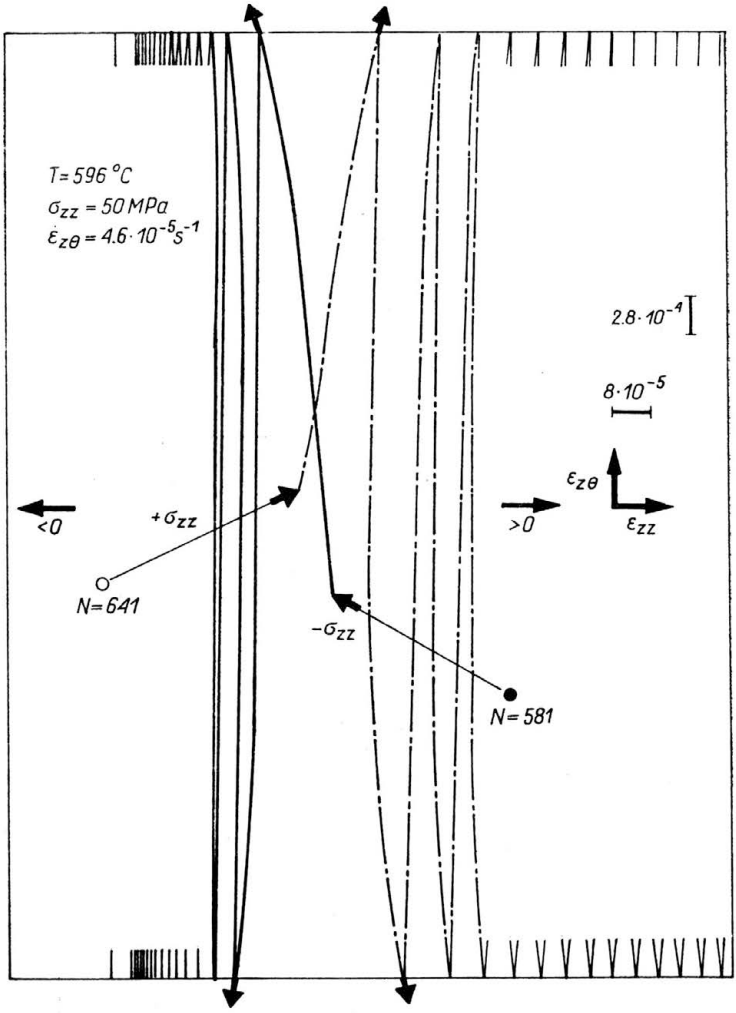

FIG. 4. Shape of the curves $\varepsilon_{z\vartheta} = f(\varepsilon_{zz})$ corresponding: a) to complete negative stress decrement ($\sigma_{zz} = -\Delta\sigma_{zz}$) (negative ratchetting) at $N = 581$. b) after an increment of stress equal at σ_{zz} at $N = 641$ (positive ratchetting).

energy lies about 5 e.V. [1]. In a similar way the saturation $\sigma_{z\vartheta}$ value for large N decreases when T increases (Figs. 2 and 3).

iv) When, after about 600 cycles, the tensile stress is removed through a σ_{zz} decrease $\Delta\sigma_{zz}$, with $\Delta\sigma_{zz} = \sigma_{zz}$, a negative ratchetting occurs ($\varepsilon_{zz} \simeq 10^{-3}$ after 100 consecutive cycles at $T = 600°C$) and must be associated with a change in the $\varepsilon_{zz} = f(\varepsilon_{z\vartheta})$ curves

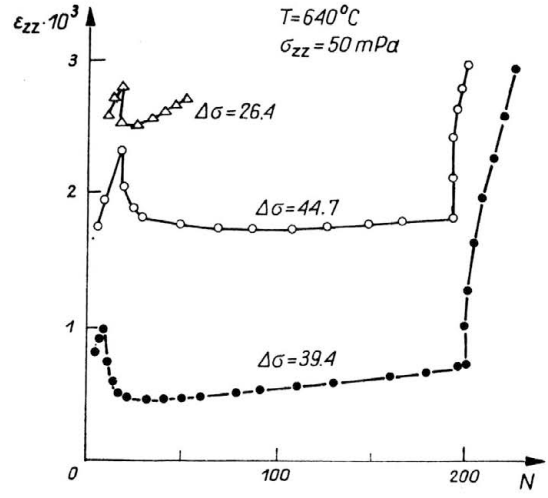

FIG. 5. Axial ratchetting responses to $\Delta\sigma_{zz}$ negative stress drops. Occurrence of successively negative, zero and positive cumulative axial strains in the curves ε_{zz} versus $(N)_T$, for various $\Delta\sigma_{zz}$.

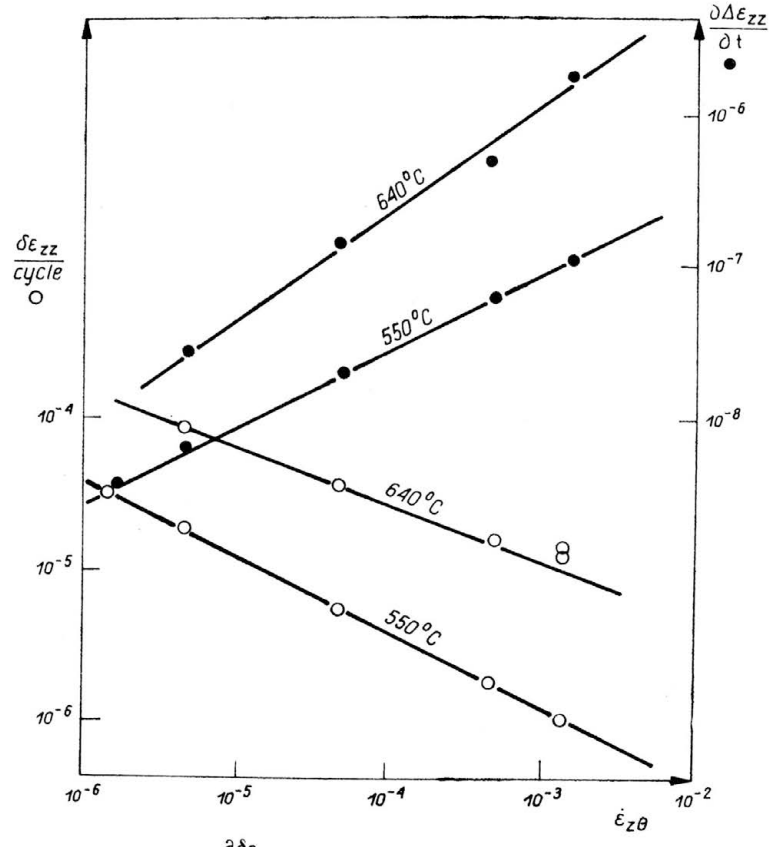

FIG. 6. Evolution of $\dot{\varepsilon}_{zz} = \dfrac{\partial \delta \varepsilon_{zz}}{\partial t}$ and $\delta\varepsilon_{zz}$ cycle with the imposed shear strain rate $\dot{\varepsilon}_{z\theta}$.

concavity, i.e. these curves are concave when $\dot{\varepsilon}_{zz} > 0$ and are convex when $\dot{\varepsilon}_{zz} < 0$ (Fig. 4).

The points iii) and iv) support the usual assumption that ratchetting phenomena are related to the rule of orthogonality of the strain flow either to equipotential surfaces (viscoplastic case) or to limit surfaces (plastic case).

v) If a partial $\Delta\sigma_{zz}$ drop leading to a new value of tensile test $(\sigma_{zz}-\Delta\sigma_{zz})$ is realized, a negative ratchetting period follows even for small drop magnitudes. This period is the longer, the larger is $\Delta\sigma_{zz}$ and is followed by a new positive ratchetting, (Fig. 5) the rate of which is close to that which would have been obtained by a direct axial loading to $(\sigma_{zz}-\Delta\sigma_{zz})$ at the same N value. This shows that the recovery of the substructure and of the associated internal variables is active even at the lowest experimental temperatures ($T = 550°C$).

vi) If, for the same type of loading, the imposed shear strain rate $\dot{\varepsilon}_{z\vartheta}$ is increased by a large amount (this was done with $\dot{\varepsilon}_{z\vartheta}$ from 1.4×10^{-6} s^{-1} to 1.4×10^{-3} s^{-1}), the tensile strain rate $\dot{\varepsilon}_{zz}$ increases while the ratchetting magnitude per cycle, $\partial\varepsilon_{zz}/\partial N$, is drastically decreased (factor $\simeq 35$) (Fig. 6). Therefore the ratchetting strain, at high temperature, $500 \leqslant T \leqslant 650°C$, is essentially viscous.

2. Comparison with a model based on proportionnel loadings

To describe tensile tests and proportionnal biaxial tensile-torsion tests, we proposed a unified viscoplastic model, the main characteristics of which are:

i) There is a single viscoplastic state equation $\bar{\dot{\varepsilon}} = f(\overline{\sigma-\alpha})$ where, $\dot{\varepsilon}_{ij}$, σ_{ij} and α_{ij} being, respectively, the strain rate components, the applied stress components and a tensorial kinematical variable, we have:

$$\bar{\dot{\varepsilon}} = \sqrt{\frac{2}{3}}\,(\dot{\varepsilon}_{ij}\dot{\varepsilon}_{ij})^{1/2}, \qquad \overline{\sigma-\alpha} = \sqrt{\frac{3}{2}}\,\{(\sigma'_{ij}-\alpha'_{ij})\,(\sigma'_{ij}-\alpha'_{ij})\}^{1/2},$$

σ'_{ij} and α'_{ij} being the deviatoric components of σ and α. The function f is strongly nonlinear, what makes it possible to obtain time dependent and time quasi-independent strains.

ii) The viscoplastic equipotentials then give strain rate components

$$\dot{\varepsilon}_{ij} = \frac{3}{2} f(\overline{\sigma-\alpha})\,\frac{\sigma'_{ij}-\alpha'_{ij}}{\overline{\sigma-\alpha}}.$$

iii) Active loadings give large strains while unloadings produce small strains; this is accounted for by a criterion depending on the internal variable α.

iv) On the unloading side of the criterion and in the tensile (or compression) uniaxial case, $\alpha = \alpha_1$, α_1 exhibiting a large strain hardening h_0. On the other side, during active loadings, $\alpha = \alpha_2 + Y$ with the corresponding H_{α_2} and H_Y hardening parameters such that $H_Y + H_{\alpha_2} \ll h_0$. In this case $\alpha_1 = \alpha$ is imposed to α_1.

v) Steady creep appears during tests and this is accounted for by recovery terms introduced in the evolution rules of α_1, α_2 and Y.

vi) The criterion is written as: $\overline{\alpha_1-\alpha_2} = Y$, $(\overline{\alpha_1-\alpha_2})$ is the second invariant of the tensor $(\alpha_1-\alpha_2)$ when complex stress states are considered. In Fig. 7 (a and b), the double space of the stresses and of the internal variables is represented. Thus the equipotential surfaces centered at $\{\alpha\} = \{\alpha_1\}$ are drawn as full line circles; they are related to the stress space and govern the strain rate direction. For instance, point A corresponds to the stress tensor $(\sigma)_1$ and, at this point, the strain rate direction is orthogonal to the circle centered at B (the representative point of $\{\alpha_1\}_1$) and passing through A.

On the other hand, the active loading-unloading criterion has a limit surface in the internal variables space represented by the dashed circle centered at $\{\alpha_2\}_1$ with a radius: $\overline{\alpha_1-\alpha_2} = Y$. The consistency equations must prevent $\{\alpha_1\}$ from lying outside the criterion limit surface (i.e. $\overline{\alpha_1-\alpha_2} > Y$ is impossible). In Fig. 7, the criterion corresponding to point A and a proportional loading (for which $\{\alpha_2\}_1$ colinear to $\{\alpha_1\}_1$) is reported.

a)

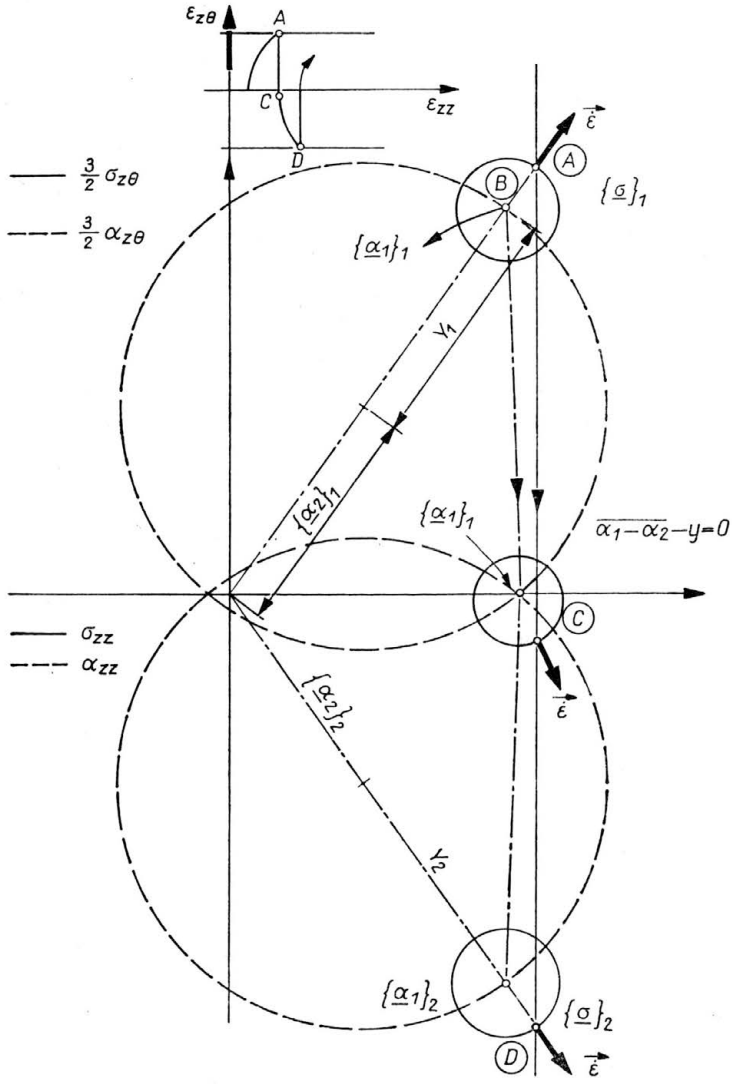

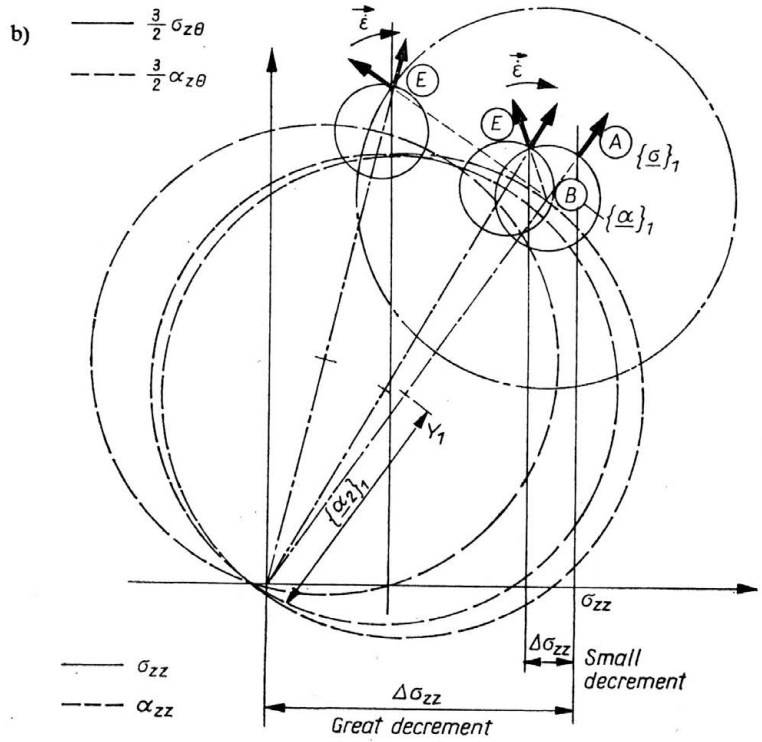

FIG. 7. Qualitative prediction of the experimental observations. a) When $\dot{\varepsilon}_{z\theta}$ changes its sign. b) For a decrement $\Delta\sigma_{zz}$ (state just after the decrement and stabilized state).

Now, let us consider the case of our experiments; to make the description simpler, Y will be assumed to be constant. If starting from point A, $\varepsilon_{z\theta}$ is cycled, $\sigma_{z\theta}$ decreases ($|\dot{\varepsilon}_{z\theta}|$ being imposed) and tends towards $-\sigma_{z\theta}$ in the steady state. When $\sigma_{z\theta}$ decreases from A, microviscoplastic strains are obtained (microviscoplastic strains are those produced in unloading situations). As h_0 is very large, $\{\alpha\} = \{\alpha_1\}$ keeps close to the applied stress $\{\sigma\}$ and a small positive axial strain is got (a limit example is given by an infinite h_0 in which case no plastic strain is produced and the criterion becomes $\overline{\sigma - \alpha_2} = Y$). This situation holds on until a point close to C is reached and $\overline{\alpha_1 - \alpha_2} = Y$ is obtained. Then, the following decrease of $\sigma_{z\theta}$ results in macroviscoplastic strains (those corresponding to active loading cases). The strain rate direction is orthogonal to the circle centered at $\{\alpha_1\}$ and passing through C. The ratchetting of axial strain is still small and positive. As the $\sigma_{z\theta}$ decrease goes on, one tends to the situation described by D, the criterion limit surface has shifted from $\{\alpha_2\}_1$ to $\{\alpha_2\}_2$.

At D ratchetting is larger as orthogonality to the circle centered at $\{\alpha_1\}_2$ and passing through $\{\sigma\}_2$ gives a larger longitudinal strain rate component. The upper left curve of Fig. 7a shows the resulting effect.

Let us now consider another type of experiment (Fig. 7b). In A, during a test, a small tensile stress decrease $\Delta\sigma_{zz}$ is produced and is such that $\sigma_{zz} - \alpha_{zz} - \Delta\sigma_{zz} < 0$, due again to the orthogonality of the flow directions to a circle which just after the drop is still centered

at A; a negative $\dot{\varepsilon}_{zz}$ is obtained during the consecutive cycling of $\varepsilon_{z\vartheta}$. The center of the flow equipotentials is no longer in A and thus in E the tensile negative strain component may be large (Fig. 7b). During the cycling α_{zz} decreases and when $\sigma_{zz}-\Delta\sigma_{zz}-\alpha_{zz} = 0$ no longitudinal ratchetting can be produced. A new positive axial ratchetting demands that internal variables recovery be active to make $\sigma_{zz}-\Delta\sigma_{zz}-\alpha_{zz} > 0$. (We present in Fig. 7b two cases of small and great decrements). Therefore the model derived and identified from proportional loading allows for qualitative predictions of the nonproportional ratchetting effects described here; this includes the important observation of a negative ratchetting following a small decrease of σ_{zz}. Quantitative comparison can therefore be continued.

References

1. P. DELOBELLE, Thesis, 1–302, Besançon 1985.
2. P. DELOBELLE, C. OYTANA, 5th Int. Sem. on: "Inelastic Analysis and Life Prediction in High Temperature Environment", Paris 1985, Rue Louis Murat Paris VIIIe, C. Baylac, A. S. Ponter and F. Leckie, EDF Septem., pp. 69–102, 1985.
3. P. DELOBELLE, D. VARCHON, Rev. Phys. Appl., **18**, 667, 1983.
4. P. BLANCHARD, J. TORTEL, 5th Int. Sem. on "Inelastic Analysis and Life Prediction in High Temperature Environment", pp. 125–186, August 26–27, Paris 1985.

LABORATOIRE DE MECANIQUE APPLIQUEE, ASSOCIE AU CNRS
FACULTE DES SCIENCES ET DES TECHNIQUES DE BESANÇON, FRANCE.

Received July 30, 1986.